High-spin states and possible chirality in the odd-A ^{133}Cs nucleus

H. Wang (王豪),[1] K. Y. Ma (马克岩),[1,2,3,*] D. Zhao (赵迪),[1] J. Y. Li (李纪元),[1] H. Y. Ye (叶欢仪),[1] X. J. Zhao (赵新洁),[1] J. X. Teng (滕佳欣),[1] Z. Qiao (乔政),[1] Y. C. Hao (郝宜春),[1] Z. H. Zhao (赵子豪),[1] H. C. Zhang (张会成),[1] Y. K. Pan (潘禹坤),[1] Y. J. Ma (马英君),[1] J. B. Lu (陆景彬),[1] Y. Zheng (郑云),[4] C. B. Li (李聪博),[4] T. X. Li (李天晓),[4] X. G. Wu (吴晓光),[4] H. Y. Wu (吴鸿毅),[4] J. Z. Li (李金泽),[4] R. Hong (洪锐),[4] Z. Y. He (贺子阳),[4] M. Zheng (郑敏),[4] and Y. Q. Li (李韵秋)[4]

[1]*College of Physics, Jilin University, Changchun 130012, China*
[2]*Chongqing Research Institute, Jilin University, Chongqing 401120, China*
[3]*Yibin Research Institute, Jilin University, Sichuan 644000, China*
[4]*China Institute of Atomic Energy, Beijing 102413, China*

(Received 25 April 2024; accepted 22 July 2024; published 5 August 2024)

High-spin states of ^{133}Cs have been studied using the fusion-evaporation reaction ^{130}Te(^{7}Li, 4n) ^{133}Cs at a beam energy of 32 MeV. The previously reported level scheme of ^{133}Cs is extended and modified with the addition of nearly 30 new γ transitions. A pair of nearly degenerate positive-parity doublet bands are identified and assigned the same $\pi d_{5/2} \otimes \nu h_{11/2}^{-2}$ configuration. The properties of both bands show general agreement with the fingerprints of chiral rotation, and thus the bands are suggested as candidate chiral doublet bands. This interpretation is also supported by the particle rotor model calculations. In addition, the high-j intruder $\pi h_{11/2}$ band is extended to the $27/2^-$ state. A new decoupled $\Delta I = 2$ sequence and a weak positive-parity band with magnetic dipole ($M1$) transitions are observed. The former is tentatively assigned the $\pi d_{5/2} h_{11/2}^2$ configuration. Meanwhile, the systematic studies of the $\pi d_{5/2}$, $\pi g_{7/2}$, and $\pi h_{11/2}$ bands in odd-A Cs isotopes are also discussed in the present work.

DOI: 10.1103/PhysRevC.110.024301

I. INTRODUCTION

Chiral symmetry exists commonly in chemistry, biology, particle physics, etc. In nuclear physics, the existence of chirality is one of the intriguing questions of high-spin nuclear structure studies, which was originally predicted by Frauendorf and Meng in 1997 [1]. A spontaneous breaking of chiral symmetry can take place in a rotating triaxial nucleus when the Fermi level lies in the lower part of valence proton (neutron) high-j (particle-like) subshell and in the upper part of valence neutron (proton) high-j (hole-like) subshell. In the laboratory frame, the restoration of the broken chiral symmetry may give rise to pairs of nearly degenerate $\Delta I = 1$ bands with the same parity, which are called chiral doublet bands [1]. So far, more than 50 candidate chiral nuclei have been reported, mainly in the $A \approx 80$ [2–4], 100 [5–9], 130 [10–29], and 190 [30–34] mass regions.

Since the first chiral doublet bands were reported in the $A \approx 130$ mass region, much effort has been made both experimentally and theoretically to investigate this phenomenon. Particularly, the $Z = 55$ Cs isotopes, wherein ^{128}Cs is proposed as the best known example revealing the chirality [19], have attracted a lot of attention. Up to now, candidate chiral doublet bands have been suggested in odd-odd nuclei ^{122,124,126,128,130,132}Cs [16–21] and odd-A nuclei ^{121,123,125,127,129,131}Cs [35–38]. As mentioned above, it is clear that the exploration for chirality in Cs isotopes has been extended to ^{132}Cs ($N = 77$) [21]. Therefore, it is interesting to investigate the systematic properties of chiral symmetry along the cesium isotopic chain to heavier nuclei. For this purpose, we try to extend the study of chiral rotation to neighboring isotope ^{133}Cs ($N = 78$), and explore the border of chirality for nuclei when the neutron number approaches the closed shell at $N = 82$.

Additionally, the known level structure of ^{133}Cs is relatively scarce, and there are still some confusions in the level scheme reported in previous works [39,40]. Thus, it is necessary to extend the information about excited states and clarify the level scheme in nucleus ^{133}Cs.

II. EXPERIMENTAL DETAILS

High-spin states in ^{133}Cs are populated through the ^{130}Te(^{7}Li, 4n) ^{133}Cs reaction. A 32 MeV ^{7}Li beam is provided by the HI-13 tandem accelerator at China Institute of Atomic Energy. The target consists of 2.96 mg/cm^2 of ^{130}Te (enriched to 99.4%) backed with 10.6 mg/cm^2 of natural Pb. A total of approximately 1.1×10^9 γ-γ coincidence events are accumulated by 24 HPGe detectors and two clover detectors during the experiment. These detectors are placed at 60°, 90°, 120°, and 150° with respect to the beam direction, respectively. In order to extract the coincidence relationships with γ rays and the multipolarities of the transitions, the data

*Contact author: mky@jlu.edu.cn

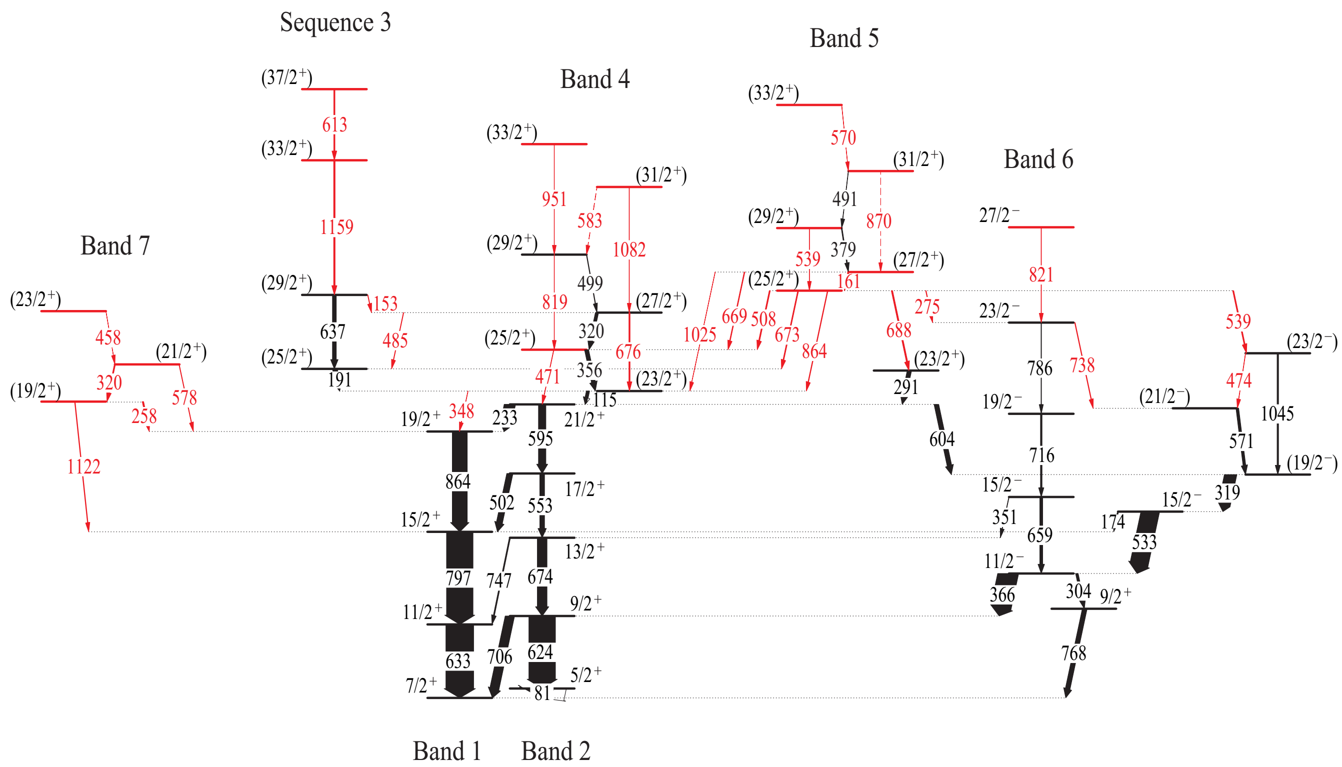

FIG. 1. Partial level scheme of ^{133}Cs deduced from the present work. Transition energies are given in keV and their measured relative intensities are proportional to the widths of the arrows. New transitions and levels are marked as red.

are sorted into a fully symmetrized γ-γ coincidence matrix and an asymmetric directional correlation ratios of oriented states (DCO) matrix. The DCO matrix is sorted with γ rays detected in the detectors at 90° on one axis and the coincident γ rays from the detectors at 150° on the other.

III. RESULTS

The partial level scheme of ^{133}Cs deduced from the present study is shown in Fig. 1. Properties and placements of all γ rays are listed in Table I. Compared with the results reported in previous works [39,40], the level scheme of ^{133}Cs is extended and modified with the addition of nearly 30 new γ transitions, including several intraband and interband transitions. The relevant details of the current level scheme will be described below.

Bands 1 and 2 have been observed and assigned as positive-parity in the previous studies [39,40], and confirmed in present work.

Sequence 3 is a newly observed structure built on the $I^{\pi} = (25/2^{+})$ state. Two new transitions of 1159 and 613 keV with the quadrupole character are observed, and thereby the spin of this structure is extended to $I^{\pi} = (37/2^{+})$. Moreover, the new linking transitions of 153 and 485 keV between the sequence 3 and band 4 are identified and added to decay path of sequence 3. A representative spectrum supporting the transitions is shown in Fig. 2(a), which depicts the spectrum gated by the 637 keV transition.

Band 4 is a positive-parity band decaying to the bands 1 and 2. In contrast to Refs. [39,40], we reverse the order of 356 and 320 keV transitions, considering that the intensity of the 356 keV transition is larger than 320 keV transition. Besides, band 4 is extended by the addition of the intraband transitions of 499 and 583 keV. Meanwhile, four new $E2$ crossover transitions of 471, 676, 819, and 1082 keV are observed, which firmly confirm the ordering of the dipole transitions of band 4, extending the band up to $I^{\pi} = (33/2^{+})$, as presented in Fig. 1.

Band 5, consisting of the cascade of 161, 379, 491, and 570 keV dipole transitions, is observed up to $I^{\pi} = (33/2^{+})$ in the present work. It is worth noting that the 324.5 keV transition reported in previous work [39] is removed on the basis of our data. Instead, new decay paths including transitions of 1025, 669, 508, 673, 864, 688, and 275 keV are established, and then the lowest observed state of band 5 is confirmed, as shown in Fig. 1. Multipolarity analysis indicates that the 1025 keV linking transition is of $\Delta I = 2$ character, and 669 and 864 keV transitions are of $\Delta I = 1$ character. Thus, band 5 is also suggested as a positive-parity band as that of band 4. Figure 2(b) shows a γ-ray coincidence spectrum supporting the proposed level scheme.

Band 6, composed of quadrupole transitions, has previously been assigned negative-parity via angular distribution analysis [39,40]. In the present experiment, one new intraband transition of 821 keV is observed and placed at the top of this band. The spectrum gated by the newly observed 821

TABLE I. The energies, relative intensities, DCO ratios, initial and final state spins, and multipolarities for transitions assigned to ^{133}Cs in the present experiment.

E_γ [a] (keV)	I_γ [b]	R_{DCO} [c]	R_{DCO} [d]	$I_i^\pi - I_f^\pi$	Multipolarity
81.0	> 100			$5/2^+ \longrightarrow 7/2^+$	$M1/E2$
114.9	41(4)		1.04(10)	$(23/2^+) \longrightarrow 21/2^+$	$(M1/E2)$
152.5	1.4(6)		0.8(3)	$(29/2^+) \longrightarrow (27/2^+)$	$(M1/E2)$
160.6	4.1(15)	0.46(18)		$(27/2^+) \longrightarrow (25/2^+)$	$(M1/E2)$
174.1	3.8(15)	0.9(3)		$15/2^- \longrightarrow 15/2^+$	$E1$
190.8	17(3)	0.52(12)		$(25/2^+) \longrightarrow (23/2^+)$	$(M1/E2)$
233.2	39(3)	0.56(6)		$21/2^+ \longrightarrow 19/2^+$	$M1/E2$
257.5	4.9(17)	0.8(3)		$(19/2^+) \longrightarrow 19/2^+$	$(M1/E2)$
275.0	1.9(8)		0.9(4)	$(25/2^+) \longrightarrow 23/2^-$	$(E1)$
291.4	15(3)	0.49(9)		$(23/2^+) \longrightarrow 21/2^+$	$(M1/E2)$
303.5	16(3)	0.56(10)		$11/2^- \longrightarrow 9/2^+$	$E1$
318.9	44(3)	0.89(6)		$(19/2^-) \longrightarrow 15/2^-$	$(E2)$
319.5	11(3)		1.0(3)	$(27/2^+) \longrightarrow (25/2^+)$	$(M1/E2)$
320.1	3.9(15)	0.44(16)		$(21/2^+) \longrightarrow (19/2^+)$	$(M1/E2)$
348.4	< 1			$(23/2^+) \longrightarrow 19/2^+$	$(E2)$
351.0	1.3(6)	0.6(3)		$15/2^- \longrightarrow 13/2^+$	$E1$
355.8	15(3)	0.53(12)		$(25/2^+) \longrightarrow (23/2^+)$	$(M1/E2)$
366.0	73.1(15)	0.63(6)		$11/2^- \longrightarrow 9/2^+$	$E1$
378.5	3.1(12)	0.6(3)		$(29/2^+) \longrightarrow (27/2^+)$	$(M1/E2)$
458.2	1.4(7)	0.6(3)		$(23/2^+) \longrightarrow (21/2^+)$	$(M1/E2)$
471.0	< 1			$(25/2^+) \longrightarrow 21/2^+$	$(E2)$
474.0	< 1			$(23/2^-) \longrightarrow (21/2^-)$	$(M1/E2)$
485.0	1.5(7)		0.9(4)	$(27/2^+) \longrightarrow (25/2^+)$	$(M1/E2)$
491.2	1.3(5)		1.1(5)	$(31/2^+) \longrightarrow (29/2^+)$	$(M1/E2)$
499.1	1.8(7)		0.9(3)	$(29/2^+) \longrightarrow (27/2^+)$	$(M1/E2)$
502.2	22(3)	0.50(9)		$17/2^+ \longrightarrow 15/2^+$	$M1/E2$
508.4	1.8(8)		1.6(8)	$(25/2^+) \longrightarrow (25/2^+)$	$(M1/E2)$
533.1	65(2)	0.95(6)		$15/2^- \longrightarrow 11/2^-$	$E2$
538.5	3.0(12)	0.7(3)		$(25/2^+) \longrightarrow (23/2^-)$	$(E1)$
539.0	< 1			$(29/2^+) \longrightarrow (25/2^+)$	$(E2)$
553.0	17(3)	1.0(2)		$17/2^+ \longrightarrow 13/2^+$	$E2$
569.6	< 1			$(33/2^+) \longrightarrow (31/2^+)$	$(M1/E2)$
571.1	7(2)	0.55(16)		$(21/2^-) \longrightarrow (19/2^-)$	$(M1/E2)$
577.8	1.5(7)	0.6(3)		$(21/2^+) \longrightarrow 19/2^+$	$(M1/E2)$
582.7	< 1			$(31/2^+) \longrightarrow (29/2^+)$	$(M1/E2)$
595.3	27(4)	1.02(19)		$21/2^+ \longrightarrow 17/2^+$	$E2$
604.3	13(2)	0.66(13)		$21/2^+ \longrightarrow (19/2^-)$	$E1$
612.5	2.6(11)	0.9(3)		$(37/2^+) \longrightarrow (33/2^+)$	$(E2)$
624.4	95.8(3)	1.07(4)		$9/2^+ \longrightarrow 5/2^+$	$E2$
632.9	100	0.93(5)		$11/2^+ \longrightarrow 7/2^+$	$E2$
637.3	11(3)	1.0(3)		$(29/2^+) \longrightarrow (25/2^+)$	$(E2)$
659.1	10(3)	1.0(2)		$15/2^- \longrightarrow 11/2^-$	$E2$
668.5	1.7(7)	0.6(3)		$(27/2^+) \longrightarrow (25/2^+)$	$(M1/E2)$
673.3	3.2(13)		2.0(7)	$(25/2^+) \longrightarrow (25/2^+)$	$(M1/E2)$
674.1	35(4)	0.94(14)		$13/2^+ \longrightarrow 9/2^+$	$E2$
675.6	4.1(16)	1.0(4)		$(27/2^+) \longrightarrow (23/2^+)$	$(E2)$
687.5	4.7(16)		1.3(5)	$(25/2^+) \longrightarrow (23/2^+)$	$(M1/E2)$
705.5	33(4)	0.67(11)		$9/2^+ \longrightarrow 7/2^+$	$M1/E2$
716.2	6(2)	0.9(3)		$19/2^- \longrightarrow 15/2^-$	$E2$
737.7	2.0(9)	0.5(2)		$23/2^- \longrightarrow (21/2^-)$	$(M1/E2)$
746.5	4.0(15)	0.49(18)		$13/2^+ \longrightarrow 11/2^+$	$M1/E2$
767.9	17(3)	0.58(12)		$9/2^+ \longrightarrow 7/2^+$	$M1/E2$
785.5	1.6(7)	0.9(4)		$23/2^- \longrightarrow 19/2^-$	$E2$
797.4	95.6(5)	1.09(7)		$15/2^+ \longrightarrow 11/2^+$	$E2$
819.0	< 1			$(29/2^+) \longrightarrow (25/2^+)$	$(E2)$
821.0	1.2(6)	0.8(4)		$27/2^- \longrightarrow 23/2^-$	$E2$

TABLE I. (*Continued.*)

E_γ [a] (keV)	I_γ [b]	R_{DCO} [c]	R_{DCO} [d]	$I_i^\pi - I_f^\pi$	Multipolarity
864.2	54(3)	1.06(10)		$19/2^+ \longrightarrow 15/2^+$	$E2$
864.4	2.2(9)		1.0(5)	$(25/2^+) \longrightarrow (23/2^+)$	$(M1/E2)$
870.0	< 1			$(31/2^+) \longrightarrow (27/2^+)$	$(E2)$
951.2	< 1			$(33/2^+) \longrightarrow (29/2^+)$	$(E2)$
1025.0	1.0(5)		1.7(7)	$(27/2^+) \longrightarrow (23/2^+)$	$(E2)$
1044.9	6.8(17)	1.1(4)		$(23/2^-) \longrightarrow (19/2^-)$	$(E2)$
1082.3	1.0(5)	0.9(4)		$(31/2^+) \longrightarrow (27/2^+)$	$(E2)$
1121.5	2.1(8)	1.2(5)		$(19/2^+) \longrightarrow 15/2^+$	$(E2)$
1159.4	5.1(16)	0.9(3)		$(33/2^+) \longrightarrow (29/2^+)$	$(E2)$

[a] The energy uncertainty is about 0.2 keV for strong transitions ($I_\gamma \geqslant 15$) and about 0.5 keV for weak transitions ($I_\gamma < 15$).
[b] Intensities are corrected for detector efficiency and normalized to 100 for the same 632.9 keV transition as in Refs. [39,40].
[c] DCO ratios from a gate on the quadrupole transition.
[d] DCO ratios from a gate on the dipole transition.

keV transition is provided in Fig. 2(c). Multipolarity analysis indicates that the 821 keV transition has quadrupole character, as can be seen from Table I. Thus, the spin of band 6 is extended from $I^\pi = 23/2^-$ to $I^\pi = 27/2^-$, and $2\hbar$ higher than the earlier work.

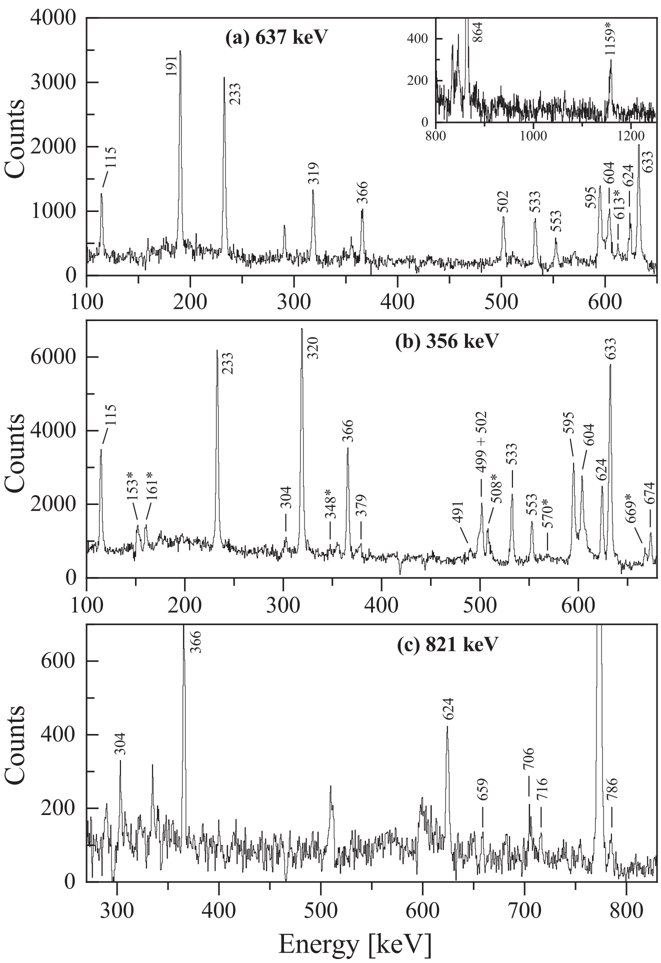

FIG. 2. γ-ray coincidence spectra gated on the (a) 637 keV, (b) 356 keV, and (c) 821 keV transitions. Inset shows the higher-energy part of the spectra. The newly identified γ rays are marked with the asterisks.

Band 7 is observed for the first time. It feeds into the positive-parity band 1 via several linking transitions. Multipolarity analysis indicates that the 1122 keV linking transition is of $\Delta I = 2$ character, and the 578 keV transition is of $\Delta I = 1$ character. Thus, band 7 is suggested as a positive-parity band as that of band 1.

IV. DISCUSSION

The positive-parity bands 1 and 2 have been reported as $\pi g_{7/2}$ and $\pi d_{5/2}$ configurations, respectively [39,40], and are suggested as a pair of pseudospin partner bands in the early work [40].

Sequence 3, consisting of $E2$ transitions, is a new structure having the positive parity. This sequence is expected to be mainly based on three-quasiparticle configuration, due to the fact that it exhibits a high excitation energy and large initial spin of $(25/2)\hbar$. Meanwhile, sequence 3 mainly decays to the $\pi d_{5/2}$ band 2 with the same parity through a strong transition of 191 keV, and thereby three-quasiparticle configuration with an odd proton particle in the $d_{5/2}$ orbital is considered for sequence 3. Additionally, the decoupled characteristic demonstrated by sequence 3 indicates that the high-j and low-Ω orbital $\pi h_{11/2}$ may be involved in its configuration. Hence, sequence 3 of ^{133}Cs is tentatively assigned the $\pi d_{5/2} h_{11/2}^2$ configuration. Indeed, similar decoupled structure with the same configuration has also been observed in neighboring isotope ^{131}Cs [41].

Band 4 decays directly to the $\pi g_{7/2}$ and $\pi d_{5/2}$ bands probably due to the alignment of the two $h_{11/2}$ neutrons [39,40], i.e., the underlying configuration being $\pi(g_{7/2}/d_{5/2}) \otimes \nu h_{11/2}^{-2}$. The newly established band 5 decays to band 4 via several dipole and quadrupole transitions, having the same positive-parity as band 4, as shown in Fig. 1. The existence of several $M1/E2$ and $E2$ linking transitions between bands 4 and 5 indicates that band 5 is likely to have the same configuration as band 4 [14,21,23]. Additionally, bands 4 and 5 lying close to each other in energy, we speculate that band 5 might be a chiral partner band of band 4. To check this conjecture,

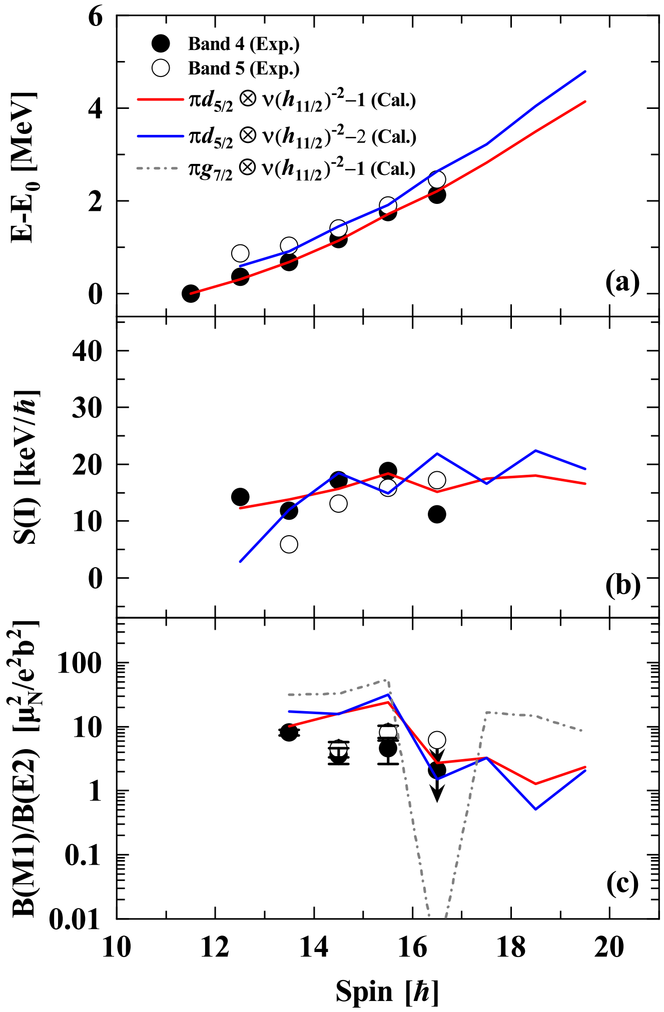

FIG. 3. (a) Experimental excitation energies $E(I)$, (b) energy staggering parameters $S(I)$, and (c) $B(M1)/B(E2)$ ratios for bands 4 and 5 in ^{133}Cs as a function of spin in comparison with the PRM calculations. The deformation parameter $\beta = 0.20$ [40] and the triaxial deformation parameter $\gamma = 31^\circ$ are adopted as input to the PRM. The energies are relative to the band head E_0 of the chiral double bands.

the fingerprints of chiral doublet bands [5,22,42,43], i.e., the excitation energies $E(I)$, energy staggering parameters $S(I) = [E(I) - E(I-1)]/2I$, and reduced transition probability ratios $B(M1)/B(E2)$ for bands 4 and 5 are extracted and presented as functions of spin in Figs. 3(a), 3(b), and 3(c), respectively.

As can be seen from Fig. 3(a), the experimental excitation energies of band 5 are slightly higher than those of band 4, and the two bands show a small energy difference within the observed spin interval. In Fig. 3(b), the doublet bands have similar $S(I)$ values, and the $S(I)$ exhibits a smooth variation versus spin. Moreover, the extracted $B(M1)/B(E2)$ ratios of bands 4 and 5 show odd-even staggering with the same phase as a function of spin in Fig. 3(c). These experimental properties are consistent with the fingerprints of chiral doublet bands [5,22,42,43]. Indeed, similar bands with the $\pi d_{5/2} \otimes \nu h_{11/2}^{-2}$ configuration have been reported as chiral doublet bands in neighboring ^{133}La nucleus [25]. Thus, the doublet bands 4 and 5 in ^{133}Cs are interpreted by the same reasoning.

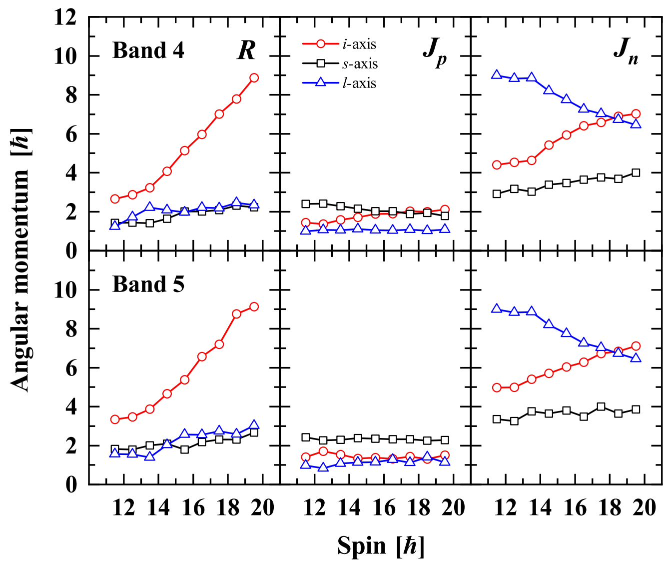

FIG. 4. The root mean square components along the intermediate (i, circles), short (s, squares), and long (l, triangles) axes of the core (R), valence proton (J_p), and valence neutrons (J_n) angular momenta calculated as functions of spin I by means of the PRM for bands 4 and 5 in ^{133}Cs.

To further examine the chirality in ^{133}Cs, calculations based on the particle rotor model (PRM) [43–49] have been performed. The calculated $E(I)$, $S(I)$, and $B(M1)/B(E2)$ ratios for positive-parity doublet bands 4 and 5 with $\pi d_{5/2} \otimes \nu h_{11/2}^{-2}$ configuration are shown in Fig. 3, in comparison with the corresponding experimental data. As illustrated in Fig. 3, the small energy differences between bands 4 and 5 are well reproduced, and the calculated $S(I)$ and $B(M1)/B(E2)$ ratios are in reasonably agreement with the experimental data. The agreement between the experimental data and theoretical calculations supports the present configuration assignment and allows us to further investigate the chiral geometry for bands 4 and 5 in ^{133}Cs.

The chiral geometry can be derived from the eigenfunctions calculated by PRM. In Fig. 4, the root mean square values of the angular momentum components of the core R, of the $d_{5/2}$ valence proton $J_p(d_{5/2})$, and of the $h_{11/2}^{-2}$ valence neutrons $J_n(h_{11/2}^{-2})$ are calculated and presented for bands 4 and 5. As can be seen, the angular momentum of the collective core for both bands 4 and 5 is aligned along the intermediate axis (i axis), which corresponds to the largest moment of inertia. Meanwhile, the angular momentum of the $d_{5/2}$ valence proton particle and the angular momentum of the $h_{11/2}^{-2}$ valence neutron holes align along the short axis (s axis) and long axis (l axis), respectively. The chiral geometry of bands 4 and 5 supports the existence of possible chiral doublet bands in ^{133}Cs.

Furthermore, in view of the mixing of $d_{5/2}$ and $g_{7/2}$ orbitals, an alternative interpretation of the bands 4 and 5, in which the odd proton occupies either the $d_{5/2}$ or the

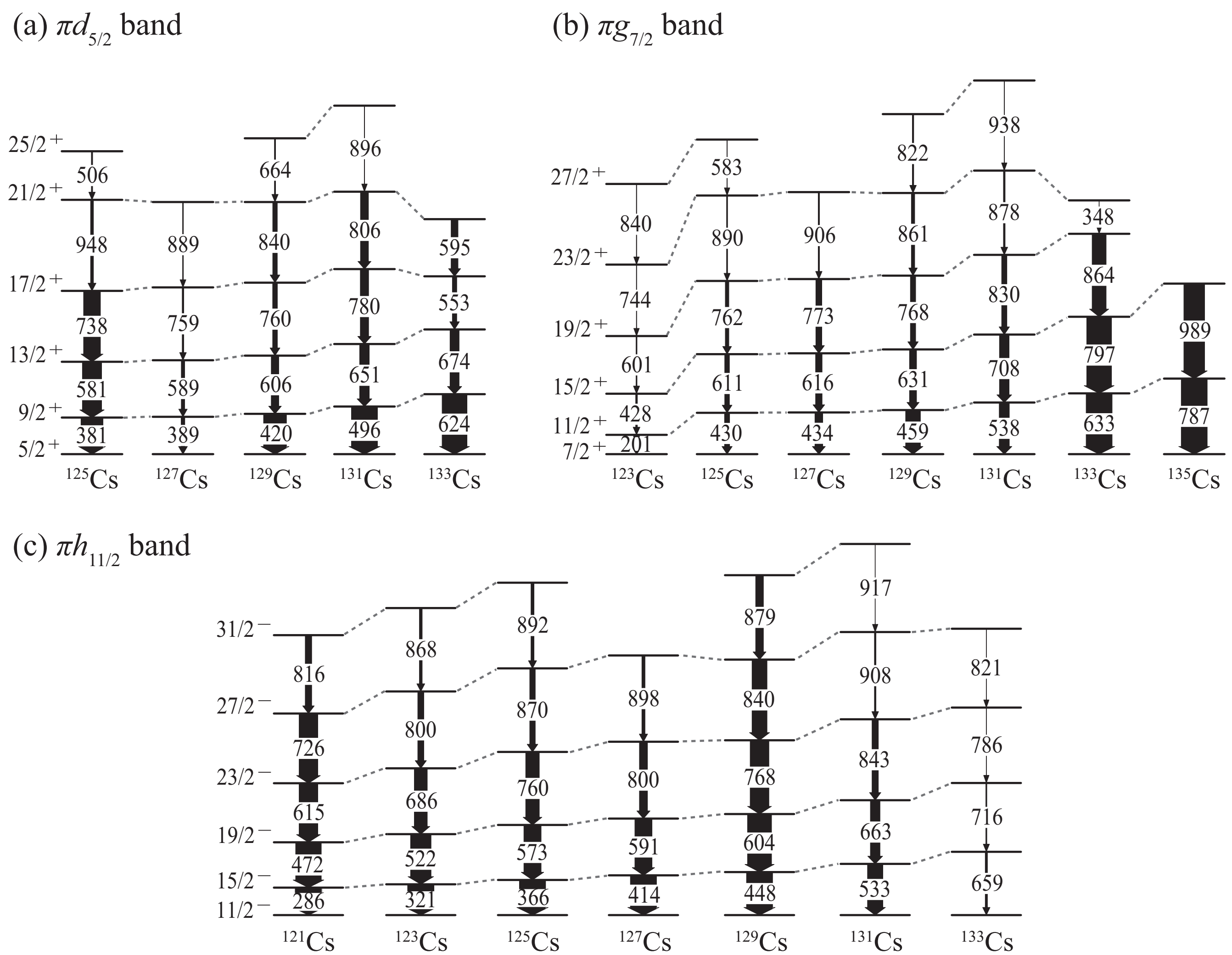

FIG. 5. Systematics comparison of $\Delta I = 2$ bands with the (a) $\pi d_{5/2}$, (b) $\pi g_{7/2}$, and (c) $\pi h_{11/2}$ configurations in the odd-A Cs isotopes. The γ-ray energies are in keV. The data of ^{133}Cs are from the present work, and of other nuclei are from Refs. [36,41,50–54].

$g_{7/2}$ orbital, should also be considered. In order to examine this hypothesis, the predicted $B(M1)/B(E2)$ ratios with the $\pi d_{5/2} \otimes \nu h_{11/2}^{-2}$ and $\pi g_{7/2} \otimes \nu h_{11/2}^{-2}$ configurations are presented in Fig. 3(c), where the calculated results using the $\pi d_{5/2} \otimes \nu h_{11/2}^{-2}$ configuration reasonably reproduce the experimental values of bands 4 and 5, while those using the $\pi g_{7/2} \otimes \nu h_{11/2}^{-2}$ configuration deviate significantly from the experimental data. Thus, we infer that the both bands are probably based on predominantly $d_{5/2}$ proton, which also supports the chiral interpretation of bands 4 and 5.

Band 6, composed of quadrupole transitions, has previously been assigned negative parity via polarization analysis [39,40]. Considering the Fermi surface for both protons and neutrons of the ^{133}Cs nucleus, band 6 built on the previously known $11/2^-$ state might be viewed as an intruder band with $\pi h_{11/2}$ character [39,40]. Band 7 decaying to band 1 is observed for the first time. This band has higher excitation energies compared with band 1, implying that band 7 is likely to be built on a multi-quasiparticle configuration.

It is worth mentioning that the $\Delta I = 2$ bands based on the $\pi d_{5/2}$, $\pi g_{7/2}$, and $\pi h_{11/2}$ configurations are observed systematically in the odd-mass cesium isotopes. To further understand the systematics of the $\Delta I = 2$ bands along the cesium isotopic chain, the level schemes of the bands are presented in Fig. 5. As illustrated in Fig. 5(a), the relative level excitation energies of the $\pi d_{5/2}$ bands increase from ^{125}Cs to ^{133}Cs till spin $13/2^+$, but decrease above those in the case of ^{133}Cs, implying that the irregular band structures start to dominate, as the neutron number approaches towards the $N = 82$ core. Indeed, similar behaviors also occur in the same-parity $\pi g_{7/2}$ bands in the odd-mass Cs isotopes, as shown in Fig. 5(b).

Figure 5(c) shows the systematics of the $\pi h_{11/2}$ bands in the odd-mass cesium isotopic chain until ^{133}Cs. The energy level spacings across the series of Cs isotopes reflect the decrease of quadrupole deformation as the neutron number increases [55–58]. Because of this, the high-j intruder $\pi h_{11/2}$ orbital moves away from the proton Fermi surface, and as a result, the $\pi h_{11/2}$ orbital becomes highly nonrast relative to $\pi d_{5/2}$ and $\pi g_{7/2}$ orbitals. It is clear from Fig. 5 that the population strength of the $\pi h_{11/2}$ band in ^{133}Cs is already significantly less than that of the $\pi d_{5/2}$ or $\pi g_{7/2}$ bands. Thus, the $\pi h_{11/2}$ band is more difficult to be populated in the heavier odd-A Cs isotope than it is in ^{133}Cs.

V. SUMMARY

Excited states of ^{133}Cs nucleus are populated by using the ^{130}Te(^{7}Li, $4n$)$\,^{133}$Cs reaction at a beam energy of 32 MeV. Compared with the previous work, the level scheme of ^{133}Cs is extended with the addition of nearly 30 new γ rays. A pair of nearly degenerate positive-parity doublet bands are identified and assigned the same $\pi d_{5/2} \otimes \nu h_{11/2}^{-2}$ configuration. The experiment excitation energies, the energy staggering parameters $S(I)$, and the $B(M1)/B(E2)$ ratios of the two bands show general agreement with the fingerprints of chiral rotation. The PRM calculations have been performed and reproduce the experimental results well, supporting the chiral interpretation of the doublet bands. In the present experiment, the high-j intruder band with $\pi h_{11/2}$ character is extended to spin $27/2^-\hbar$. A new decoupled $\Delta I = 2$ sequence and a weak positive-parity band consisting of magnetic dipole transitions are observed, and the decoupled sequence is tentatively assigned the $\pi d_{5/2} h_{11/2}^2$ configuration. Furthermore, the systematics of the $\pi d_{5/2}$, $\pi g_{7/2}$, and $\pi h_{11/2}$ bands in odd-A Cs isotopes are also investigated in the present work.

ACKNOWLEDGMENTS

This work is supported by the Jilin Scientific and Technological Development Program (Grant No. 20230101009JC); the National Natural Science Foundation of China (Grants No. 12175086, No. 11775098, No. U1867210, and No. 11405072); the Natural Science Foundation of Chongqing, China (Grant No. CSTB2022NSCQMSX0315); the Natural Science Foundation of Sichuan, China (Grant No. 23NSFSC1051); and the Graduate Innovation Fund of Jilin University (Grant No. 2023CX051).

[1] S. Frauendorf and J. Meng, Nucl. Phys. A **617**, 131 (1997).

[2] S. Y. Wang, B. Qi, L. Liu, S. Q. Zhang, H. Hua, X. Q. Li, Y. Y. Chen, L. H. Zhu, J. Meng *et al.*, Phys. Lett. B **703**, 40 (2011).

[3] C. Liu, S. Y. Wang, R. A. Bark, S. Q. Zhang, J. Meng, B. Qi, P. Jones, S. M. Wyngaardt, J. Zhao *et al.*, Phys. Rev. Lett. **116**, 112501 (2016).

[4] C. Liu, S. Y. Wang, B. Qi, S. Wang, D. P. Sun, Z. Q. Li, R. A. Bark, P. Jones, J. J. Lawrie *et al.*, Phys. Rev. C **100**, 054309 (2019).

[5] C. Vaman, D. B. Fossan, T. Koike, K. Starosta, I. Y. Lee, and A. O. Macchiavelli, Phys. Rev. Lett. **92**, 032501 (2004).

[6] J. A. Alcántara-Núñez, J. R. B. Oliveira, E. W. Cybulska, N. H. Medina, M. N. Rao, R. V. Ribas, M. A. Rizzutto, W. A. Seale, F. Falla-Sotelo, K. T. Wiedemann, V. I. Dimitrov, and S. Frauendorf, Phys. Rev. C **69**, 024317 (2004).

[7] P. Joshi, D. G. Jenkins, P. M. Raddon, A. J. Simons, R. Wadsworth, A. R. Wilkinson, D. B. Fossan, T. Koike, K. Starosta *et al.*, Phys. Lett. B **595**, 135 (2004).

[8] S. J. Zhu, J. H. Hamilton, A. V. Ramayya, J. K. Hwang, J. O. Rasmussen, Y. X. Luo, K. Li, J. G. Wang, X. L. Che *et al.*, Chin. Phys. C **33**, 256 (2009).

[9] M. Wang, Y. Y. Wang, L. H. Zhu, B. H. Sun, G. L. Zhang, L. C. He, W. W. Qu, F. Wang, T. F. Wang *et al.*, Phys. Rev. C **98**, 014304 (2018).

[10] S. Mukhopadhyay, D. Almehed, U. Garg, S. Frauendorf, T. Li, P. V. M. Rao, X. Wang, S. S. Ghughre, M. P. Carpenter, S. Gros, A. Hecht, R.V.F. Janssens, F. G. Kondev, T. Lauritsen, D. Seweryniak, and S. Zhu, Phys. Rev. Lett. **99**, 172501 (2007).

[11] A. D. Ayangeakaa, U. Garg, M. D. Anthony, S. Frauendorf, J. T. Matta, B. K. Nayak, D. Patel, Q. B. Chen, S. Q. Zhang *et al.*, Phys. Rev. Lett. **110**, 172504 (2013).

[12] C. M. Petrache, B. F. Lv, A. Astier, E. Dupont, Y. K. Wang, S. Q. Zhang, P. W. Zhao, Z. X. Ren, J. Meng *et al.*, Phys. Rev. C **97**, 041304(R) (2018).

[13] C. M. Petrache, S. Frauendorf, M. Matsuzaki, R. Leguillon, T. Zerrouki, S. Lunardi, D. Bazzacco, C. A. Ur, E. Farnea *et al.*, Phys. Rev. C **86**, 044321 (2012).

[14] K. Starosta, T. Koike, C. J. Chiara, D. B. Fossan, D. R. LaFosse, A. A. Hecht, C. W. Beausang, M. A. Caprio, J. R. Cooper *et al.*, Phys. Rev. Lett. **86**, 971 (2001).

[15] Z. Yan-Xin, T. Komatsubara, Y. J. Ma, Y. H. Zhang, S. Y. Wang, Y. Z. Liu, and K. Furuno, Chin. Phys. Lett. **26**, 082301 (2009).

[16] Y.-N. U, S. J. Zhu, M. Sakhaee, L. M. Yang, C. Y. Gan, L. Y. Zhu, R. Q. Xu, X. L. Che, M. L. Li *et al.*, J. Phys. G: Nucl. Part. Phys. **31**, B1 (2005).

[17] K. Selvakumar, A. K. Singh, C. Ghosh, P. Singh, A. Goswami, R. Raut, A. Mukherjee, U. Datta, P. Datta *et al.*, Phys. Rev. C **92**, 064307 (2015).

[18] E. Grodner, I. Sankowska, T. Morek, S. G. Rohozinski, C. Droste, J. Srebrny, A. A. Pasternak, M. Kisielinski, M. Kowalczyk *et al.*, Phys. Lett. B **703**, 46 (2011).

[19] E. Grodner, J. Srebrny, A. A. Pasternak, I. Zalewska, T. Morek, C. Droste, J. Mierzejewski, M. Kowalczyk, J. Kownacki *et al.*, Phys. Rev. Lett. **97**, 172501 (2006).

[20] A. J. Simons, P. Joshi, D. G. Jenkins, P. M. Raddon, R. Wadsworth, D. B. Fossan, T. Koike, C. Vaman, K. Starosta *et al.*, J. Phys. G: Nucl. Part. Phys. **31**, 541 (2005).

[21] G. Rainovski, E. S. Paul, H. J. Chantler, P. J. Nolan, D. G. Jenkins, R. Wadsworth, P. Raddon, A. Simons, D. B. Fossan *et al.*, Phys. Rev. C **68**, 024318 (2003).

[22] T. Koike, K. Starosta, C. J. Chiara, D. B. Fossan, and D. R. LaFosse, Phys. Rev. C **67**, 044319 (2003).

[23] T. Koike, K. Starosta, C. J. Chiara, D. B. Fossan, and D. R. LaFosse, Phys. Rev. C **63**, 061304(R) (2001).

[24] K. Y. Ma, J. B. Lu, D. Yang, H. D. Wang, Y. Z. Liu, X. G. Wu, Y. Zheng, and C. Y. He, Phys. Rev. C **85**, 037301 (2012).

[25] C. M. Petrache, Q. B. Chen, S. Guo, A. D. Ayangeakaa, U. Garg, J. T. Matta, B. K. Nayak, D. Patel, J. Meng *et al.*, Phys. Rev. C **94**, 064309 (2016).

[26] R. A. Bark, A. M. Baxter, A. P. Byrne, G. D. Dracoulis, T. Kibédi, T. R. McGoram, and S. M. Mullins, Nucl. Phys. A **691**, 577 (2001).
[27] J. Timár, K. Starosta, I. Kuti, D. Sohler, D. B. Fossan, T. Koike, E. S. Paul, A. J. Boston, H. J. Chantler, M. Descovich, R. M. Clark, M. Cromaz, P. Fallon, I. Y. Lee, A. O. Macchiavelli, C. J. Chiara, R. Wadsworth, A. A. Hecht, D. Almehed, and S. Frauendorf, Phys. Rev. C **84**, 044302 (2011).
[28] A. A. Hecht, C. W. Beausang, K. E. Zyromski, D. L. Balabanski, C. J. Barton, M. A. Caprio, R. F. Casten, J. R. Cooper, D. J. Hartley *et al.*, Phys. Rev. C **63**, 051302(R) (2001).
[29] S. Guo, C. M. Petrache, D. Mengoni, Y. H. Qiang, Y. P. Wang, Y. Y. Wang, J. Meng, Y. K. Wang, S. Q. Zhang *et al.*, Phys. Lett. B **807**, 135572 (2020).
[30] D. L. Balabanski, M. Danchev, D. J. Hartley, L. L. Riedinger, O. Zeidan, J.-Y. Zhang, C. J. Barton, C. W. Beausang, M. A. Caprio, R. F. Casten, J. R. Cooper, A. A. Hecht, R. Krucken, J. R. Novak, N. V. Zamfir, and K. E. Zyromski, Phys. Rev. C **70**, 044305 (2004).
[31] J. Ndayishimye, E. A. Lawrie, O. Shirinda, J. L. Easton, S. M. Wyngaardt, R. A. Bark, S. P. Bvumbi, T. R. S. Dinoko, P. Jones *et al.*, Acta Phys. Pol. B **48**, 343 (2017).
[32] P. L. Masiteng, E. A. Lawrie, T. M. Ramashidzha, J. J. Lawrie, R. A. Bark, R. Lindsay, F. Komati, J. Kau, P. Maine *et al.*, Eur. Phys. J. A **50**, 119 (2014).
[33] E. A. Lawrie, P. A. Vymers, C. Vieu, J. J. Lawrie, C. Schuck, R. A. Bark, R. Lindsay, G. K. Mabala, S. M. Maliage *et al.*, Eur. Phys. J. A **45**, 39 (2010).
[34] B. W. Xiong and Y. Y. Wang, At. Data Nucl. Data Tables **125**, 193 (2019).
[35] K. Singh, S. Sihotra, S. S. Malik, J. Goswamy, D. Mehta, N. Singh, R. Kumar, R. P. Singh, S. Muralithar *et al.*, Eur. Phys. J. A **27**, 321 (2006).
[36] S. Sihotra, K. Singh, S. S. Malik, J. Goswamy, R. Palit, Z. Naik, D. Mehta, N. Singh, R. Kumar *et al.*, Phys. Rev. C **79**, 044317 (2009).
[37] R. Guo, W. J. Sun, J. Li, D. Yang, Y. Liu, C. Ru, and J. Chi, Phys. Rev. C **100**, 034328 (2019).
[38] D. Chen, J. Li, and R. Guo, Eur. Phys. J. A **59**, 142 (2023).
[39] S. Biswas, R. Palit, J. Sethi, S. Saha, A. Raghav, U. Garg, M. S. R. Laskar, F. S. Babra, Z. Naik *et al.*, Phys. Rev. C **95**, 064320 (2017).
[40] Q. Xu, Z. G. Xiao, S. J. Zhu, C. Qi, H. Jia, B. Qi, R. S. Wang, W. J. Cheng, Y. Zhang *et al.*, Eur. Phys. J. A **54**, 83 (2018).
[41] S. Sihotra, R. Palit, Z. Naik, K. Singh, P. K. Joshi, A. Y. Deo, J. Goswamy, S. S. Malik, D. Mehta *et al.*, Phys. Rev. C **78**, 034313 (2008).
[42] T. Koike, K. Starosta, C. Vaman, T. Ahn, D. B. Fossan, R. M. Clark, M. Cromaz, I. Y. Lee, and A. O. Macchiavelli, Sensitive criterion for chirality; chiral doublet bands In $^{104}Rh_{59}$, AIP Conf. Proc. **656**, 160 (2003).
[43] T. Koike, K. Starosta, and I. Hamamoto, Phys. Rev. Lett. **93**, 172502 (2004).
[44] J. Peng, J. Meng, and S. Q. Zhang, Phys. Rev. C **68**, 044324 (2003).
[45] S. Y. Wang, S. Q. Zhang, B. Qi, and J. Meng, Phys. Rev. C **75**, 024309 (2007).
[46] S. Q. Zhang, B. Qi, S. Y. Wang, and J. Meng, Phys. Rev. C **75**, 044307 (2007).
[47] S. Y. Wang, S. Q. Zhang, B. Qi, J. Peng, J. M. Yao, and J. Meng, Phys. Rev. C **77**, 034314 (2008).
[48] B. Qi, S. Q. Zhang, J. Meng, S. Y. Wang, and S. Frauendorf, Phys. Lett. B **675**, 175 (2009).
[49] B. Qi, S. Q. Zhang, S. Y. Wang, J. Meng, and T. Koike, Phys. Rev. C **83**, 034303 (2011).
[50] C. B. Moon, T. Komatsubara, and K. Furuno, J. Korean Phys. Soc. **38**, 83 (2001).
[51] K. Singh, Z. Naik, R. Kumar, J. Goswamy, D. Mehta, N. Singh, C. R. Praharaj, E. S. Paul, K. P. Singh *et al.*, Eur. Phys. J. A **25**, 345 (2005).
[52] J. Sun, Y. J. Ma, T. Komatsubara, K. Furuno, Y. H. Zhang, W. P. Zhou, S. Y. Wang, X. Y. Hu, H. Guo *et al.*, Phys. Rev. C **93**, 064301 (2016).
[53] Y. Liang, R. Ma, E. S. Paul, N. Xu, D. B. Fossan, and R. A. Wyss, Phys. Rev. C **42**, 890 (1990).
[54] N. Fotiades, J. A. Cizewski, K. Higashiyama, N. Yoshinaga, E. Teruya, R. Krucken, R. M. Clark, P. Fallon, I. Y. Lee *et al.*, Phys. Rev. C **88**, 064315 (2013).
[55] X. Sun, Z. Liu, X. Zhou, X. Lei, H. Jin, Q. Pan, Y. Zhang, Y. Guo, Y. Luo *et al.*, Phys. Rev. C **51**, 2803 (1995).
[56] S. M. Qaim, Nucl. Phys. A **154**, 145 (1970).
[57] U. Garg, T. P. Sjoreen, and D. B. Fossan, Phys. Rev. C **19**, 207 (1979).
[58] R. Garg, S. Kumar, M. Saxena, S. Goyal, D. Siwal, S. Verma, R. Palit, S. Saha, J. Sethi *et al.*, Phys. Rev. C **87**, 034317 (2013).